Positron emission tomography imaging analysis of G2A as a negative modifier of lymphoid leukemogenesis initiated by the BCR-ABL oncogene

Lu Q. Le,[1,5] Janusz H.S. Kabarowski,[1] Stephane Wong,[1] Khoi Nguyen,[2,3] Sanjiv S. Gambhir,[2,3] and Owen N. Witte[1,2,4,6]

[1]Department of Microbiology, Immunology, and Molecular Genetics
[2]Department of Molecular and Medical Pharmacology
[3]Crump Institute for Molecular Imaging
[4]Howard Hughes Medical Institute
[5]Medical Scientist Training Program
University of California, Los Angeles
Los Angeles, California 90095
[6]Correspondence: owenw@microbio.ucla.edu

Summary

G2A is a lymphocyte-expressed G protein-coupled receptor whose genetic ablation results in the development of autoimmunity. Using HSV-TK reporter gene directed positron emission tomography (PET), we demonstrate that prior to any indication of the onset of illness, mice transplanted with BCR-ABL transduced G2A-deficient bone marrow harbor expanded populations of leukemic cells compared to recipients of wild-type bone marrow. The target cell type and anatomical locations of leukemia development are indistinguishable in animals transplanted with G2A+/+ or G2A−/− cells. Shorter disease latency in the G2A-deficient background is associated with an increased rate of cellular expansion. PET can be successfully applied to the temporal and spatial analysis of Bcr-Abl driven leukemic progression and should have utility for the study of other leukemias and lymphomas.

Introduction

The presence of identical disease associated genetic mutations within the human population often results in quite different individual outcomes with respect to susceptibility, latency, clinical features, and severity (Houlston and Tomlinson, 1998). Similarly, mice inheriting the same genetic mutation predisposing to certain diseases may show very different outcomes, attributed to differences in genetic background and the influence of one or more modifier genes. Identification of these modifiers provides important insights into developmental and physiological processes, and genetic studies remain the most powerful tool with which to do so (Nadeau, 2001).

The development of cancer results from the progressive accumulation of mutations which ultimately lead to the deregulation of normal cellular growth, survival, and differentiative mechanisms. Cancer susceptibility and progression in human and mouse populations is governed by a complex set of genetic traits which includes modifier loci (Balmain, 2002; Van Dyke and Jacks, 2002). Several modifier loci have subsequently been mapped further to define individual modifier genes. Notable examples are the association of genetic polymorphisms within the genes encoding secretory phospholipase A_2 ($sPLA_2$) and the $p16^{INK4a}$ cyclin-dependent kinase inhibitor products which confer strain dependent susceptibility to intestinal tumorigenesis and plasmacytoma induction, respectively (Cormier et al., 1997; Dietrich et al., 1993; Mock et al., 1993; Zhang et al., 2001).

Classical approaches to study the impact of candidate modifier genes upon cancer progression in animal models are limited by the requirement for autopsy to evaluate tumor burden, which necessitates manual exploration of multiple anatomical sites for tumor incidence and imposes a requirement for large experimental groups to control for intersubject variability. Live imaging of cancer progression by techniques such as positron emission

SIGNIFICANCE

Expression of the BCR-ABL tyrosine kinase is the initiating etiological event in a subset of human lymphoid leukemias. We have developed a transplantation model for BCR-ABL induced lymphoid tumorigenesis utilizing positron emission tomography to study the modification of leukemogenic progression caused by loss of a novel BCR-ABL transcriptional target, the G protein-coupled receptor G2A. This receptor represents a class of lymphoid growth regulators which modifies the action of oncogenic signals from BCR-ABL. This model allows the kinetic and spatial examination of leukemia initiation and progression in individual animals and the separate contribution of proliferative expansion and leukemic dissemination to these processes. We believe that this system can be further applied to more thoroughly evaluate therapeutic agents targeting specific pathways deregulated by BCR-ABL and other leukemia specific oncoproteins.

tomography (PET) would circumvent these problems and allow sequential kinetic and spatial measurements of tumor development in individual animals.

BCR-ABL is a chimeric tyrosine kinase resulting from a reciprocal translocation of chromosomes 22 and 9, producing a fusion product from the cellular genes encoding BCR and c-ABL (Chopra et al., 1999; Nowell and Hungerford, 1960; Rowley, 1973). In patients, three fusion products are detected, each differing in the amount of BCR encoded sequences they contain. P185 BCR-ABL is associated with 15%–25% of patients with aggressive, poor prognostic acute lymphoblastic leukemia (ALL), and P210 BCR-ABL is associated with 95% of cases of chronic myeloid leukemia (CML). The more recently identified P230 BCR-ABL is associated with a mild chronic neutrophilic leukemia (Saglio et al., 1990; Sawyers, 1999). The etiology of BCR-ABL+ leukemia has received considerable attention due to the tremendous efficacy with which the ABL kinase inhibitory drug Gleevec® (STI571) induces disease remission in CML patients (Druker and Lydon, 2000). However, recent reports of clinical resistance to this drug developing in a proportion of patients have underlined the need for further studies of its pathopharmacological actions in vivo (Gorre et al., 2001).

Clinical studies and experimental animal models are consistent with BCR-ABL serving as the initiating event in the transformation/leukemogenic process and with additional genetic, and perhaps epigenetic, events being required for progression to overt malignancy (Gishizky and Witte, 1992; Mitelman, 1993; Sawyers, 1999). The latency for Pre-B lymphoma induction by the related viral oncoprotein vABL has been shown to be highly mouse strain dependent (Abelson and Rabstein, 1970; Risser et al., 1978; Rosenberg and Baltimore, 1976). While 90% of neonatal BALB/c mice injected intraperitoneally with Abelson Murine Leukemia Virus (Abl-MLV) develop lymphomas with a mean latent period of 92 days, only 36% of B6 mice develop a similar malignancy with a protracted latent period of 120 days (Risser et al., 1985). This implies that genetic context plays a major role governing the susceptibility to disease induced by the ABL family of oncoproteins.

We have previously identified a novel G protein-coupled receptor (GPCR), named G2A, in a search for genes transcriptionally regulated by P185 BCR-ABL (Weng et al., 1998). G2A belongs to a subfamily of GPCR with ligand specificities for structurally related lysophospholipids (Im et al., 2001; Kabarowski et al., 2001; Xu et al., 2000; Zhu et al., 2001). G2A is expressed predominantly in hematopoietic cells including T and B lymphocytes. Forced overexpression of G2A antagonizes the transformation potency of BCR-ABL in vitro (Weng et al., 1998). G2A-deficient mice develop a late onset, slowly progressive autoimmune syndrome, demonstrating a critical role for G2A in controlling peripheral lymphocyte homeostasis, T lymphocyte proliferation and autoimmunity (Le et al., 2001). These observations support the notion that G2A negatively regulates lymphocyte growth responses in the context of sustained proliferative signals.

In this study, we have sought to determine by a direct genetic test whether loss of G2A function modulates the efficiency of BCR-ABL leukemogenesis. We found that mice transplanted with BCR-ABL transduced G2A-deficient bone marrow cells exhibit earlier tumor onset, more rapid tumor progression, and shorter survival times compared to those receiving BCR-ABL transduced wild-type bone marrow. Based on our knowledge of signaling and biological properties of G2A (Kabarowski et al., 2000; Le et al., 2001; Weng et al., 1998), this may be due to altered leukemic cell migration/homing or more rapid cell-cycle progression. To address this issue, we utilized positron emission tomography (PET) based on coexpression of the HSV-TK reporter gene to evaluate tumor extent and sites of tumor growth in a kinetic manner for individual mice transplanted with BCR-ABL transduced wild-type or G2A-deficient bone marrow cells.

PET is a nuclear imaging technique that combines high image resolution with a quantitative method for detecting the location and levels of radiotracer accumulation in living subjects (Cherry and Gambhir, 2001). Bone marrow cells were transduced with a bicistronic retroviral vector containing BCR-ABL and the HSV-TKsr39 allele as a PET reporter gene whose product will sequester positron-emitting reporter probes (Herschman et al., 2000). The selective retention of the PET probe in target tissues is then imaged in living animals, allowing one to generate consecutive, quantitative, and spatial measurements showing the dynamic evolution of tumor development in a noninvasive fashion. We found that prior to any indication of overt illness (preleukemic phase), mice transplanted with G2A-deficient bone marrow harbor significantly expanded populations of BCR-ABL positive B lymphoid progenitor cells compared to recipients of wild-type bone marrow. However, the spatial pattern of disease development is similar in all animals, suggesting that the decreased latency for leukemogenesis in the context of G2A ablation results primarily from increased leukemic cell expansion, rather than altered cellular migration and sites of leukemic dissemination. These results indicate that G2A is a negative modifier of lymphoid leukemogenesis induced by BCR-ABL in vivo acting primarily to affect cell proliferation or viability.

Results

Effect of G2A ablation on P185 BCR-ABL-mediated transformation in vitro

The transformation activities of P185 BCR-ABL include the ability to eliminate growth factor requirements of bone marrow B cell progenitors for survival and proliferation (McLaughlin et al., 1987, 1989). As G2A is transcriptionally induced in B lymphoid progenitors by BCR-ABL during this transformation process and suppresses its transformation potency when overexpressed (Weng et al., 1998), we wished to determine whether induction of G2A expression under physiological conditions plays a role in BCR-ABL in vitro transformation.

Retrovirally mediated expression of BCR-ABL in primary bone marrow results in transformation of Pro/Pre-B cells in stromal cell-dependent cultures (McLaughlin et al., 1987). The growth rate of Pre-B cells from infected marrow can be directly monitored and quantitatively reflects BCR-ABL tyrosine kinase activity and transformation potency (Lugo et al., 1990). To determine the effect of G2A ablation on P185 BCR-ABL-mediated transformation in vitro, bone marrow cells from wild-type and G2A-deficient mice were infected with a retrovirus encoding green fluorescent protein (GFP) plus P185 BCR-ABL (MSCV-GFP-IRES-BCR-ABL). Liquid cultures were plated in triplicate and monitored for Pre-B cell outgrowth at various time points. All infected cultures, irrespective of genotype, gave rise to mor-

phologically typical transformed Pro/Pre-B lymphocytes (Figures 1A and 1B). Since forced overexpression of G2A at high levels suppressed the transformation potency of BCR-ABL in fibroblasts and decreased lymphoid transformation (Weng et al., 1998), we predicted that lack of G2A function might enhance BCR-ABL transformation potency in long-term bone marrow culture (LTBMC). Surprisingly, cell counts performed on these cultures revealed that both wild-type and G2A-deficient Pre-B lymphocytes expanded at similar rates (Figure 1C). These results indicate that G2A-deficient bone marrow cells are equally susceptible to P185 BCR-ABL-mediated transformation in vitro, with comparable rates of cellular expansion compared to wild-type bone marrow cells.

Loss of G2A function accelerates lymphoid leukemogenesis induced by P185 BCR-ABL

We sought to further characterize the biological properties of G2A in vivo as a more stringent test of its physiological role in BCR-ABL transformation. Although the absence of G2A expression has no effect on the transformation potency of P185 BCR-ABL in vitro, G2A may deregulate a biological process in vivo that is not adequately recapitulated in long-term bone marrow cultures. In addition, some genetic alterations that result in transformation of cultured cells do not elicit tumorigenesis in mice, and many mutations that cause dramatic effects in vivo induce no observable phenotypes in vitro. For example, while the absence of p53 has no effect on the frequency of bone marrow transformation by Abl-MLV in vitro, p53-deficient mice infected with Abl-MLV develop lymphoid tumors more rapidly compared to those which retain p53 function (Unnikrishnan et al., 1999).

P185 BCR-ABL was used to induce lymphoid leukemogenesis in a retroviral infection and transplantation model (Afar et al., 1997; Lim et al., 2000). This model was chosen because it is highly reproducible and the kinetics of leukemia induction are well established. In order to avoid host immune responses to the human P185 BCR-ABL protein, we used SCID mice as recipients of transduced bone marrow cells (Stripecke et al., 1998).

Wild-type or G2A-deficient bone marrow cells were infected with retroviruses encoding GFP plus BCR-ABL (MSCV-GFP-IRES-P185 BCR-ABL) followed by transplantation of transduced cells into sublethally irradiated C.B-17$^{SCID/SCID}$ mice. In four independent experiments (25 mice per group total), we consistently observed that SCID mice transplanted with infected G2A-deficient bone marrow cells displayed a marked acceleration of leukemia development. These animals began to exhibit signs of illness characterized by hind limb paralysis, hunchback, tachypnea, and eventually death 19 days following transplantation, with 50% mortality at 33 days. By 50 days, all animals transplanted with BCR-ABL transduced G2A-deficient bone marrow cells had succumbed to leukemia. In contrast, all mice reconstituted with BCR-ABL transduced wild-type bone marrow cells survived to day 31, with only 5% mortality by 33 days, and 55% mortality at 51 days (Figure 2). All animals were sacrificed shortly thereafter. These data demonstrate that although initial in vitro transformation events elicited by P185 BCR-ABL are not affected by loss of G2A function, loss of G2A function potentiates the development of P185 BCR-ABL induced leukemia in vivo.

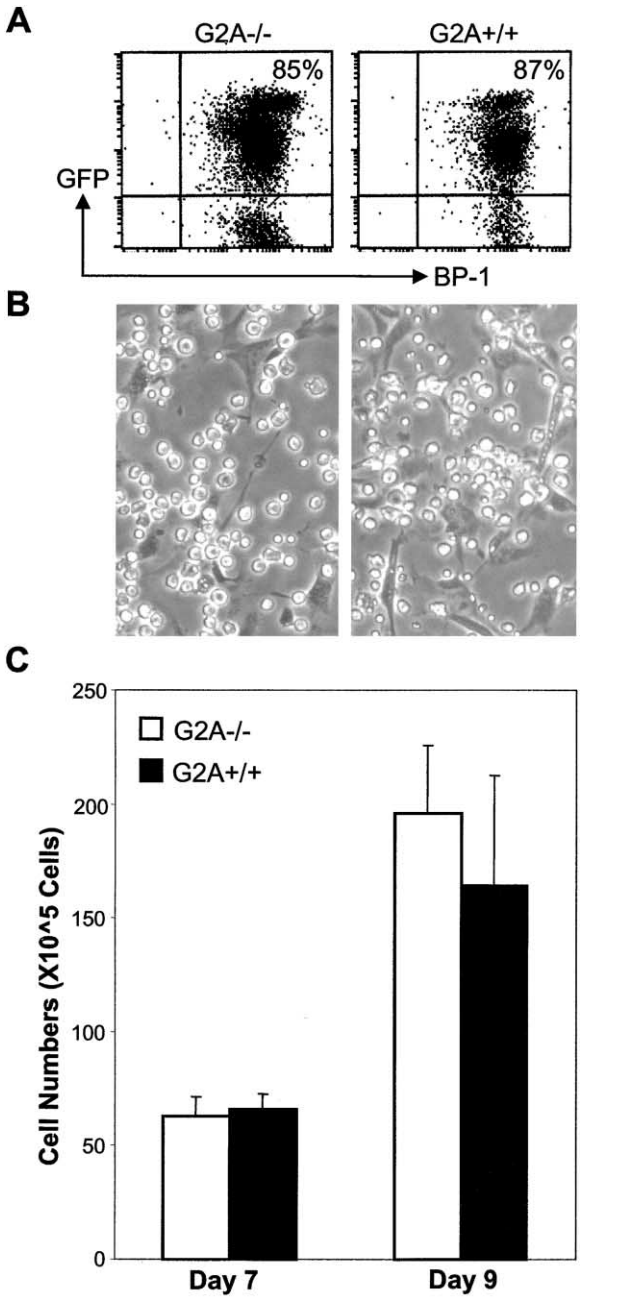

Figure 1. Absence of G2A does not affect in vitro transformation efficiency of P185BCR-ABL

Bone marrow cells from G2A-deficient and wild-type littermates were infected with MSCV-GFP-IRES-P185 BCR-ABL retroviruses and plated in liquid culture. **A:** Flow cytometric analysis of G2A-deficient (left) and wild-type (right) transformed bone marrow cells. BP-1 is a surface marker for Pre/Pro-B cells (Cooper et al., 1986). Proportions of cells in each quadrant are indicated as percentages. **B:** Photomicrographs (magnification 40×) of G2A-deficient (left) and wild-type (right) transformed Pre-B lymphocytes. **C:** Pre-B cell growth was monitored at the indicated timepoints. Mean cell count values from triplicate data sets are presented with standard deviations. Cultures reached confluency around 2×10^7 cells/per 3 ml culture.

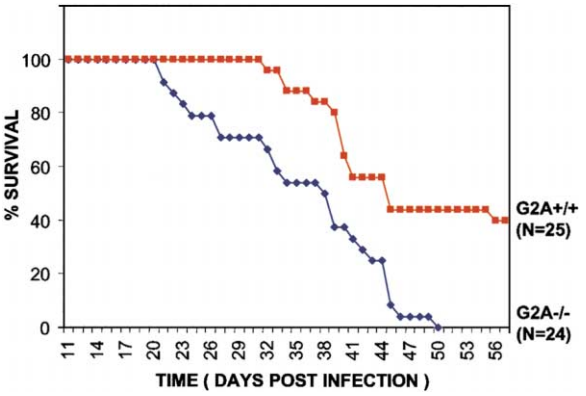

Figure 2. Acceleration of P185 BCR-ABL mediated lymphoid leukemogenesis in the absence of G2A

Bone marrow cells from either G2A-deficient or wild-type mice were infected with MSCV-GFP-IRES-P185 BCR-ABL retroviral stocks. 1×10^6 infected cells were intravenously injected into the tail vein of sublethally irradiated SCID mice. Mice were monitored for signs of illness daily. Experiment was terminated after two months. Leukemic diagnosis of newly deceased mice was based on gross, microscopic, and FACS analyses. Survival data are presented as a Kaplan-Meyer plot.

Mice transplanted with P185 BCR-ABL transduced wild-type and G2A-deficient bone marrow develop leukemias of identical phenotype

To determine if loss of G2A function alters BCR-ABL mediated leukemogenesis by affecting the target cell specificity for transformation, we examined whether P185 BCR-ABL-induced leukemias that developed in wild-type and G2A-deficient backgrounds had similar phenotypes. We performed gross clinical and cellular analyses of overtly ill mice. These studies revealed comparable pathology, independent of genetic status (Figure 3A). Disease symptoms were uniform regardless of genotype, typically including high peripheral white blood cell counts, splenomegaly, bone marrow involvement, asymmetric lymph node enlargement, and hind limb paralysis. In all cases, histochemical analysis of affected mice showed high grade lymphoblastic lymphomas that were morphologically and histologically indistinguishable in mice receiving BCR-ABL transduced wild-type or G2A-deficient bone marrow cells (Figures 3B–3D). RT-PCR analysis of RNA from G2A-deficient leukemic cells derived from bone marrows and spleens of multiple animals failed to detect the expression of G2A mRNA. However, its expression is abundant in wild-type leukemic cells (Figure 3E).

To determine the lineage and developmental stage of leukemias arising in recipients, tumor cells were isolated from bone marrow, spleen, lymph nodes, and peripheral blood, and analyzed by flow cytometric analysis of specific surface markers. Leukemic cells of both genotypes in 100% of terminally ill mice were uniformly GFP-positive and positive for B220 and BP-1 markers, consistent with a Pro/Pre-B cell phenotype (Cooper et al., 1986; Hardy and Hayakawa, 2001) (Figures 4A–4C). In addition, leukemic cells were negative for Thy1.2, Ter119, and Gr-1 markers. Thus, the combination of histological and flow cytometric analyses indicate that mice reconstituted with BCR-ABL transduced bone marrow cells of either genotype succumb to similar Pro/Pre-B cell leukemias. Therefore, loss of G2A function enhances BCR-ABL mediated leukemogenesis without affecting the target cell for transformation.

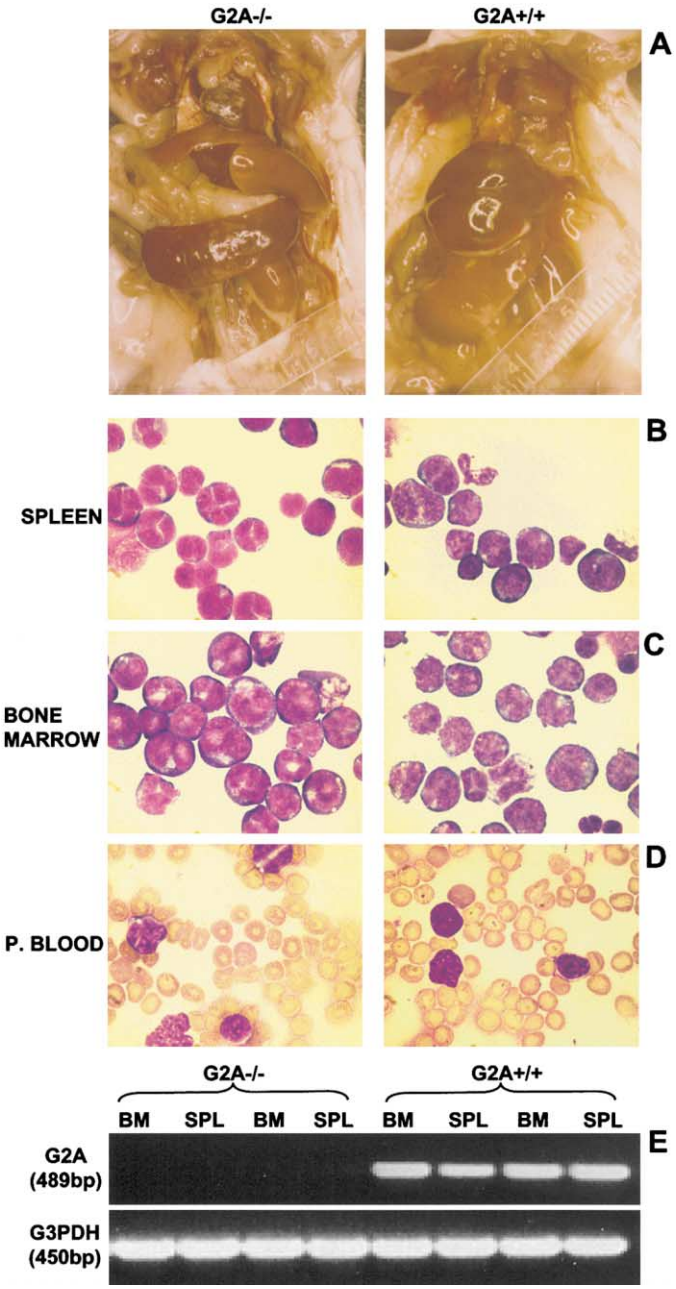

Figure 3. Comparison of the leukemic histopathology in recipients of wild-type and G2A-deficient bone marrow cells

A: Enlarged spleens from typical leukemic mice reconstituted with G2A-deficent bone marrow (left) and its wild-type counterpart (right). **B–D:** photomicrographs (magnification 400×) of Giemsa/Wright stained G2A-deficient (left) and wild-type (right) leukemic cells derived from spleens (**B**), bone marrow (**C**), and peripheral blood smears (**D**). **E:** RT-PCR analysis using G2A-specific primers (Weng et al., 1998) of total RNA isolated from G2A-deficient (G2A−/−) or wild-type (G2A+/+) leukemic cells derived from bone marrow (BM) or spleen (SPL).

Kinetic analysis of leukemia development by PET

We previously reported that ectopic expression of G2A in heterologous cell types delays cell-cycle progression through G2/M

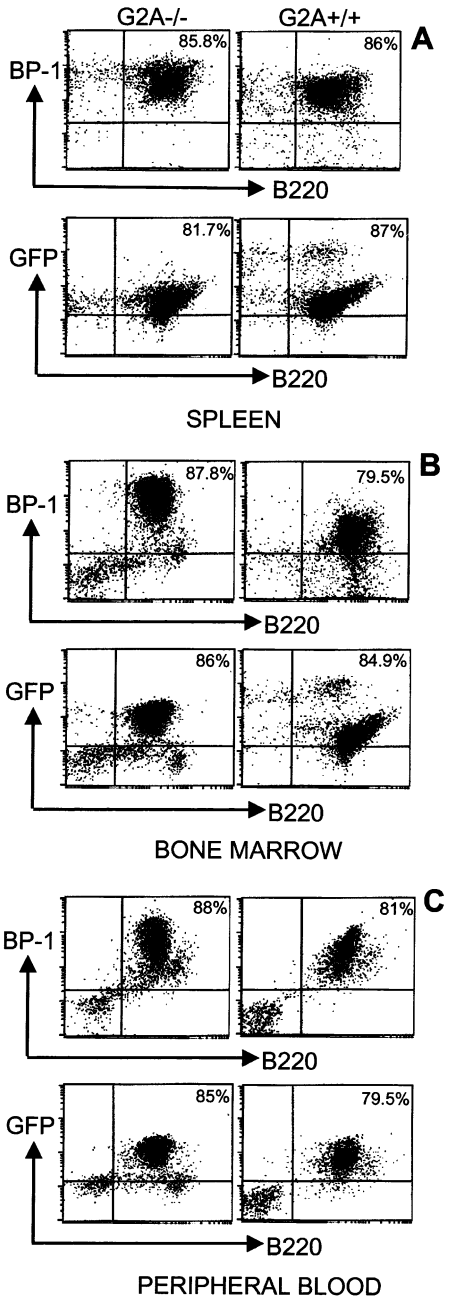

Figure 4. Flow cytometric analysis of wild-type and G2A-deficient leukemic cells

Flow cytometric analysis to determine the lineage and developmental stage of leukemias. Spleen (**A**), bone marrow (**B**), and peripheral blood (**C**) were harvested from typical leukemic mice transplanted with G2A-deficient (left) or wild-type (right) bone marrow. All leukemic cells were uniformly GFP-positive and positive for B220 and BP-1, which are markers for Pro/Pre-B cell. Proportions of cells in each quadrant are indicated as percentages.

(Weng et al., 1998). Consistent with this observation, G2A-deficient T cells are hyperproliferative to a variety of stimuli (Le et al., 2001). In addition, we have established the coupling of G2A to Gα13, leading to activation of RhoA and actin stress fiber formation in fibroblasts (Kabarowski et al., 2000). These observations implicate a number of possible roles for G2A, including negative regulation of proliferation and integration of extracellular signals with cytoskeletal reorganization and cell motility. Thus, although the cellular target for tumor induction by BCR-ABL is similar in both G2A-deficient and wild-type backgrounds, G2A ablation could have a profound effect on the rate of proliferation, migratory behavior, or anatomical colonization of leukemic cells in vivo. We therefore examined the contribution of altered leukemic cell migration/homing versus cell-cycle progression to the earlier mortality associated with loss of G2A function.

We exploited PET technology to follow kinetic and spatial characteristics of leukemia development in individual mice transplanted with BCR-ABL transduced wild-type or G2A-deficient bone marrow cells. To achieve this goal, we coupled the expression of P185 BCR-ABL to that of the Herpes Simplex Virus (HSV)-1sr39TK PET reporter gene in a bicistronic retroviral vector (MSCV-TK-IRES-P185 BCR-ABL) (Figure 5A). HSV-1sr39TK is a specific mutant form of Herpes Simplex Virus Thymidine Kinase (TK) that has a significantly higher affinity for the acycloguanosines (Gambhir et al., 2000). To demonstrate the ability to image transplanted MSCV-TK-IRES-P185 BCR-ABL transduced wild-type bone marrow cells in recipient SCID mice, we compared SCID mice transplanted with either MSCV-GFP-IRES-P185 BCR-ABL or MSCV-TK-IRES-P185 BCR-ABL transduced bone marrow cells (Figure 5A). Twenty-five days following transplantation, recipient SCID mice were injected intravenously with 200 μCi 9-(4-[^{18}F]-fluoro-3 hydroxymethylbutyl) guanine (FHBG) and subjected to whole-body microPET scan. Serial 3D microPET scans were performed dorsoventrally with data collection in 64 planes of section, and mice were also X-rayed for visualization of skeletal landmarks following the final scan. Physiological hepato-biliary and renal excretion of FHBG is seen in several planes in all recipient animals (Figures 5B and 5C). Therefore, interpretations of PET scan are most informative for the thorax, neck, head, and limbs. Multiple consecutive sections at the thoracic spine level of a TK-BCR-ABL-positive leukemic animal are shown in Figure 5D to demonstrate the 3D resolution of the microPET technique.

SCID mice were transplanted with wild-type or G2A-deficient bone marrow cells transduced with MSCV-TK-IRES-P185 BCR-ABL retroviruses. 9, 16, 23, and 30 days following transplantation, mice were injected intravenously with 200 μCi FHBG and subjected to whole-body microPET scan. Serial 3D microPET scans were performed dorsoventrally with data collection in 64 planes of section. We successfully imaged highly specific regional expansion of B lymphoid cells in these mice at times when few leukemic cells were detectable in their peripheral blood. Representative images derived from data collected in three sectional planes of multiple (2–5) animals per group at each timepoint are presented (Figures 6A–6D). Although no PET signal was detected 9 days following transplantation of either BCR-ABL transduced G2A-deficient or BCR-ABL transduced wild-type bone marrow cells (Figure 6A), strong signals were observed in recipients of BCR-ABL transduced G2A-deficient bone marrow cells in the spine and calvaria at day 16. At the same time, no signal was observed in recipients of BCR-ABL transduced wild-type bone marrow (Figure 6B). By day 23, TK$^+$ G2A-deficient cells had accumulated in the cervical lymph nodes, sternum, and femur/tibia as indicated by intense signals detected in these areas (Figure 6C). In contrast, at this timepoint, a weak signal was detected in the thoracic spine area of recipi-

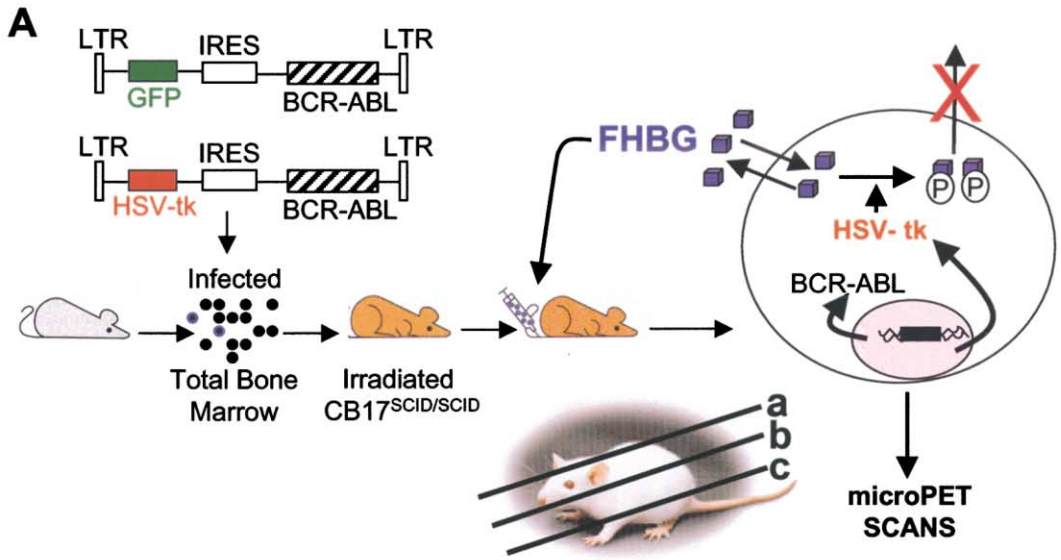
A
LTR
IRES
LTR
GFP
BCR-ABL
LTR
IRES
LTR
HSV-tk
BCR-ABL
Infected
Total Bone Marrow
Irradiated CB17SCID/SCID
FHBG
HSV- tk
BCR-ABL
a
b
c
microPET SCANS

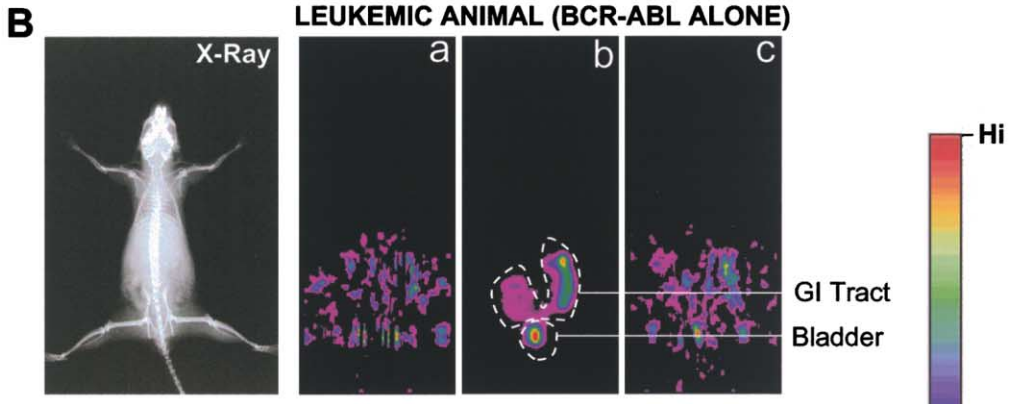
B
LEUKEMIC ANIMAL (BCR-ABL ALONE)
X-Ray
a
b
c
GI Tract
Bladder
Hi
Lo

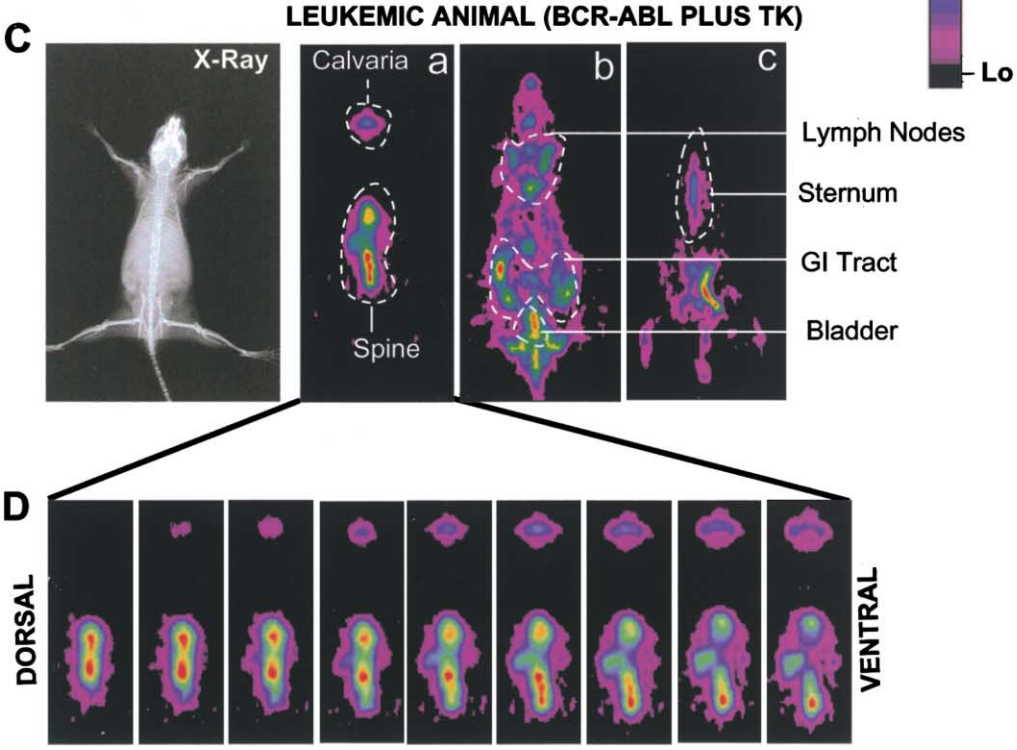
C
LEUKEMIC ANIMAL (BCR-ABL PLUS TK)
X-Ray
Calvaria
a
b
c
Lymph Nodes
Sternum
GI Tract
Bladder
Spine
D
DORSAL
VENTRAL

ents of BCR-ABL transduced wild-type bone marrow cells. Thirty days posttransplantation, TK^+ wild-type leukemic cells eventually extended to the calvaria, cervical lymph nodes, sternum, and femur (Figure 6D). However, at this timepoint, the PET signal was weaker compared to that observed in recipients of BCR-ABL transduced G2A-deficient bone marrow cells.

These observations indicate that the initiation and progression of disease is significantly accelerated in mice receiving MSCV-TK-IRES-P185 BCR-ABL transduced G2A-deficient bone marrow cells. However, the pattern and anatomical locations of leukemia development were indistinguishable in all animals tested, suggesting that increased mortality of mice transplanted with BCR-ABL transduced G2A-deficient bone marrow is associated with increased cellular expansion and resultant leukemic burden, rather than an altered route of leukemic dissemination and organ/tissue involvement.

Discussion

The ability to noninvasively visualize tumor development in animal models has become a major area of cancer research. We have developed a novel transplantation model for BCR-ABL induced leukemia in which expression of BCR-ABL is coupled to that of the Herpes Simplex Virus 1sr39 thymidine kinase PET reporter gene. This model allows the kinetic and spatial examination of leukemia initiation and progression in individual animals and the separate contribution of proliferative expansion and leukemic dissemination to these processes. Our ability to successfully monitor leukemia development in individual recipient mice by microPET imaging validates the use of this model of BCR-ABL induced leukemia for the study of candidate modifiers and effector pathways. We therefore applied this model to address whether the G protein-coupled receptor G2A, a transcriptional target of BCR-ABL, modifies leukemogenesis induced by this oncoprotein.

Although G2A function is dispensable for normal T and B lymphopoiesis throughout young adulthood, G2A-deficient T lymphocytes exhibit hyperproliferative responses in vitro, and G2A-deficient mice develop a slowly progressive systemic autoimmune syndrome (Le et al., 2001). While these observations have supported a role for G2A as a negative regulator of lymphocyte growth responses, our present studies extend the biological context in which this property is manifest to include oncogenic transformation. G2A is a powerful negative modifier of P185 BCR-ABL mediated leukemogenesis. Mice transplanted with BCR-ABL transduced G2A-deficient bone marrow cells exhibit earlier tumor onset, more rapid tumor progression, and shorter survival times compared to those receiving BCR-ABL transduced wild-type bone marrow cells. Interestingly, despite a dramatic effect on the kinetics of leukemogenesis in vivo, loss of G2A function has no discernable effect on B lymphoid transformation by BCR-ABL in LTBMCs in vitro. These results suggest that G2A regulates a biological process in vivo that is not adequately recapitulated in long-term bone marrow cultures.

Although the precise molecular basis underlying the modification of BCR-ABL mediated leukemogenesis by G2A is presently unknown, several possible explanations can be proposed based on our knowledge of the biological properties of this receptor. We recently identified the inflammatory lysophospholipid lysophosphatidylcholine (LPC) as a ligand for G2A (Kabarowski et al., 2001), and it is possible that high concentrations of LPC or other cofactors in vivo work through G2A to limit lymphocyte growth. G2A may thereby constitute a transcriptionally regulated negative feedback loop utilized by cells as a global protective mechanism to balance sustained proliferative stimuli. Transcriptional induction of Smad 7 by TGFβ and Suppressor Of Cytokine Signaling (Socs) proteins in reponse to cytokine receptor activation serve as paradigms for the activation of a negative growth regulatory pathway by positive growth signals (Krebs and Hilton, 2001; Nakao et al., 1997).

It is possible that transcriptional induction of G2A in BCR-ABL expressing B lymphoid progenitors elicits signals that specifically antagonize one or more of those mediating key pathophysiological processes downstream of BCR-ABL. In this respect, the ability of BCR-ABL to decrease the adhesive capacity of hematopoietic progenitors to stromal elements is believed to contribute to their escape from normal growth inhibitory influences within the bone marrow microenvironment and abnormal homing to extramedullary sites (Gordon et al., 1987a, 1987b). This property is associated with the ability of BCR-ABL to associate with the actin cytoskeleton (McWhirter and Wang, 1993) and target the Rho family GTPase RAC (Skorski et al., 1998). G2A also modifies cytoskeletal organization and cellular adhesion by activating RhoA leading to assembly of actin stress fibers and focal adhesion contacts (Kabarowski et al., 2000). Coordinate regulation of Rho family GTPases (CDC42, RAC, RhoA) is critical for the normal regulation of cellular adhesive and migratory behavior (Nobes and Hall, 1995; Sander et al., 1999), suggesting that G2A may modify the leukemogenic potency of BCR-ABL by altering cellular migratory/homing or proliferative properties through the concurrent deregulation of RAC and RhoA activities.

To address these possibilities, we utilized PET to simultaneously examine cellular expansion and migratory characteristics in individual preleukemic mice. We observed that prior to any indication of overt illness, mice transplanted with G2A-deficient bone marrow harbor significantly expanded populations of leukemic cells compared to recipients of wild-type bone marrow.

Figure 5. Overview of PET technique

A: Schematic representation of the protocol for PET imaging of preleukemic mice. SCID mice were transplanted with wild-type total bone marrow cells infected with MSCV-GFP-IRES-P185 BCR-ABL or MSCV-1sr39TK-IRES-P185 BCR-ABL retroviral stocks. 25 days following transplantation, recipient SCID mice were administered 200 μCi of [^{18}F] FHBG fluoropenciclovir and subsequently subjected to serial microPET scans dorsoventrally. Representative examples of microPET scan images of 3 sectional planes a, b, and c from (**B**) a control leukemic SCID mouse (BCR-ABL alone) and (**C**) a TK^+ leukemic SCID mouse (BCR-ABL plus TK). Anatomical landmarks are marked with white broken lines. Following the final scan, mice were X-rayed for identification of anatomical landmarks. Physiological bowel and renal excretions of the radiolabeled probe represent background and are seen in both control and TK^+ animals. Signals of TK-labeled tumor cells are detected in the spine, calvarium, and lymph node areas of leukemic animals. Multiple consecutive dorsoventral sections at the thoracic spine level of a TK^+ leukemic animal are shown in **D**. The scans are normalized to the individual maximum for each mouse. The color scale represents the relative intensity from low (Lo) to high (Hi) of positron emission from FHBG.

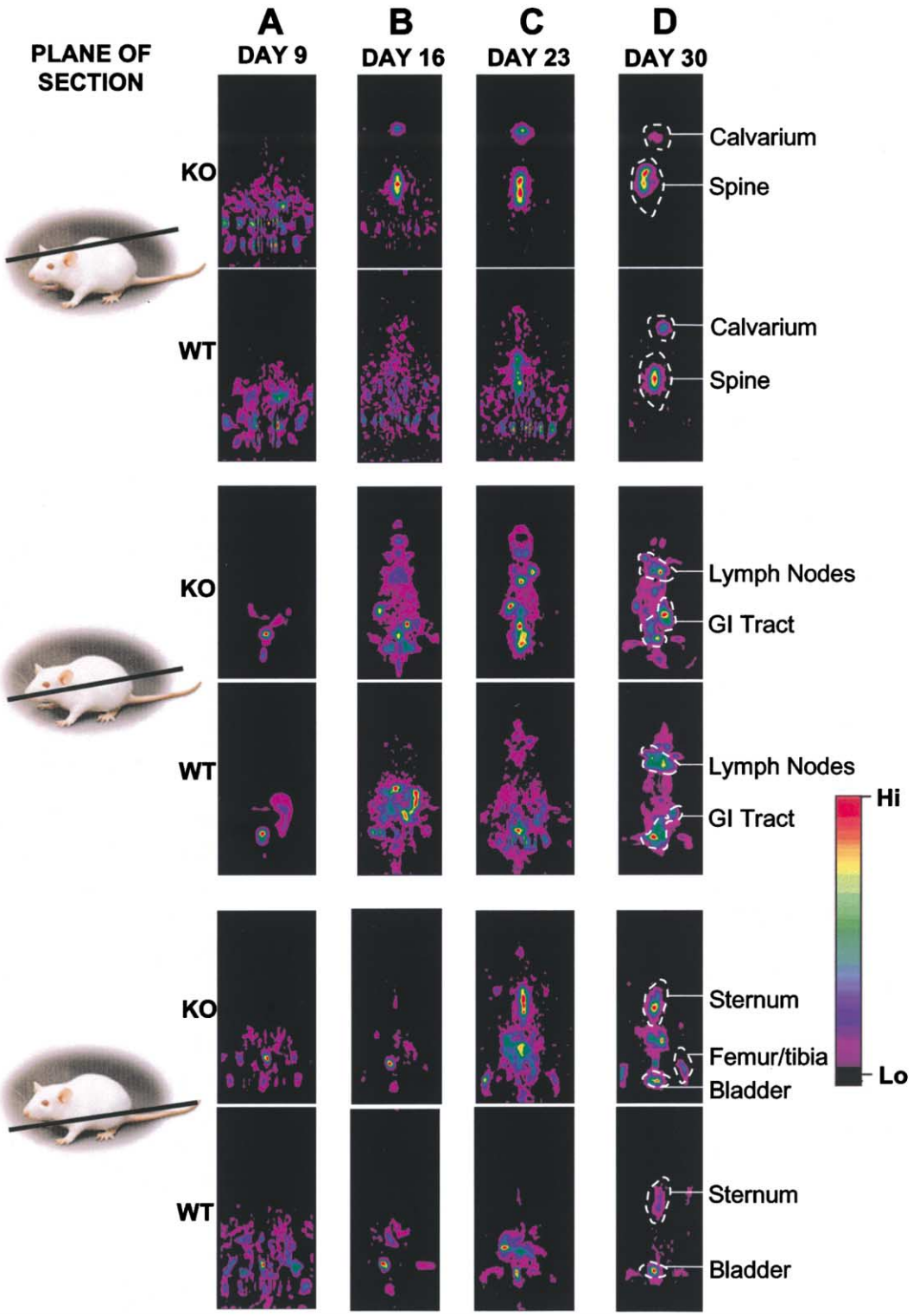

Figure 6. Serial microPET images of preleukemic and leukemic mice

SCID mice were transplanted with either wild-type or G2A-deficient total bone marrow cells infected with MSCV-1sr39TK-IRES-P185 BCR-ABL retroviruses and subjected to microPET scan 9 (**A**), 16 (**B**), 23 (**C**), and 30 (**D**) days posttransplantation. Representative images at each timepoint are presented. Anatomical landmarks are marked with white broken lines. Upper panels: coronal sections of microPET images at the spine level of recipients of MSCV-1sr39TK-IRES-P185 BCR-ABL transduced G2A-deficient (top) and MSCV-1sr39TK-IRES-P185 BCR-ABL transduced wild-type (bottom) bone marrow cells. Middle panels: as for upper panels, except coronal section is taken at the gastrointestinal level. Lower panels: as for upper panels, except coronal section is taken at the sternum level. The scans are normalized to the individual maximum for each mouse. The color scale represents the relative intensity from low (Lo) to high (Hi) of positron emission from FHBG.

However, the anatomical sites of disease development are similar in all animals, suggesting that the increased mortality of mice transplanted with BCR-ABL transduced G2A-deficient bone marrow is likely associated with increased cellular expansion and resultant leukemic burden, rather than altered leukemic dissemination and organ/tissue involvement.

G2A exhibits a high degree of homology to several other GPCRs, most notably TDAG8, GPR4, and OGR1, which are coexpressed in lymphocytes (Choi et al., 1996; Heiber et al., 1995; Xu and Casey, 1996) and share ligand specificities toward structurally related lysophospholipids (Im et al., 2001; Kabarowski et al., 2001; Xu et al., 2000; Zhu et al., 2001). Interestingly, the human genes encoding G2A, TDAG8, and OGR1 are located on chromosome 14q32, a region in which abnormalities are frequently found in lymphoid proliferative disorders and lymphomas (Kyaw et al., 1998; Weng et al., 1998). We detect a high level of G2A mRNA expression in multiple human Ph-positive cell lines (unpublished data). Future studies will address the question of whether alterations in expression or specific mutations, translocation, and/or rearrangements within the G2A locus are associated with the progression of human Ph-positive lymphoid leukemias.

In conclusion, G2A functions as a negative modifier of BCR-ABL induced leukemogenesis. By adapting a murine transplantation model of BCR-ABL induced leukemia for microPET imaging, we have developed a system with the potential to study preleukemic events and resolve the contribution of candidate cellular and biological processes otherwise inseparable in animal model systems evaluated by autopsy alone. In this regard, loss of G2A function primarily affects the early proliferative expansion of B lymphoid cells in the bone marrow. Such models should allow more thorough evaluation of therapeutic agents with respect to their impact on both cell expansion and sites of leukemia development.

Experimental procedures

Mice

G2A-deficient mice were generated via disruption of the G2A locus by homologous recombination in 129SvJ embryonic stem (ES) cells as previously described (Le et al., 2001). Heterozygotes carrying the G2A null mutation were intercrossed, and offspring were genotyped by Southern blot analysis of tail DNA to identify homozygous mutant mice. All studies reported in this manuscript were conducted with mice backcrossed 5 generations onto the BALB/c background. C.B-17$^{SCID/SCID}$ mice (Custer et al., 1985) were obtained from Taconic (Germantown, New York) and housed in isolated barrier facilities containing autoclaved food, water, bedding, and cages. All other animals were housed in the conventional animal facility at UCLA (Los Angeles, California). Animal care and use is in compliance with regulations of the Chancellor's Animal Research Committee (ARC) at UCLA.

Retroviral vectors and generation of virus stocks

The retroviral vector pMSCV was used (Hawley et al., 1994). P185 BCR-ABL cDNA was ligated with the encephalomyocarditis virus Internal Ribosome Entry Site (IRES) (CLONTECH, Palo Alto, CA) and then cloned into pMSCV. Green Fluorescent Protein (CLONTECH) or HSV-1sr39TK was inserted into pMSCV at a unique EcoRI site between the 3′ LTR and IRES-P185 BCR-ABL encoding sequences to generate MSCV-GFP-IRES-BCR-ABL and MSCV-1sr39TK-IRES-P185 BCR-ABL, respectively. HSV-1sr39TK was a gift from Dr. Margaret Black (Washington State University) (Gambhir et al., 2000).

Retroviral stocks were prepared by transient cotransfection of 293T cells with retroviral vectors and Psi− ecotropic packaging vector (Muller et al., 1991). Supernatants were collected 24–48 hr posttransfection. The same retroviral stock was used to infect bone marrow cells from either G2A-deficient or wild-type mice.

Bone marrow transformation and in vivo leukemogenesis assay

Bone marrow cells were freshly isolated from the tibias and femurs of 4–8 week old G2A-deficient or wild-type littermates. Bone marrow cells were subsequently infected with MSCV-GFP-IRES-BCR-ABL retroviruses and plated in triplicate in 6 cm dishes as previously described (McLaughlin et al., 1987). The numbers of nonadherent Pre-B cells were counted 7–9 days postinfection.

For in vivo leukemogenesis assays, 6–8 week old severe combined immunodeficient (SCID) mice were sublethally irradiated with 275 rads one day prior to reconstitution. Whole bone marrow from G2A-deficient or wild-type littermates was isolated and infected with retroviruses as described above. Three hours after infection, bone marrow cells were injected intravenously by tail vein into recipient SCID mice. Animals were monitored daily for signs of illness for two months as previously described (Afar et al., 1997; Lim et al., 2000). For PET imaging of leukemic animals, whole bone marrow from G2A-deficient or wild-type littermates was infected with MSCV-HSV-1sr39TK-IRES-P185 BCR-ABL retroviral stocks and transplanted into SCID mice as described above.

Histological analysis

Spleen, bone marrow, and blood were harvested from overtly ill animals and single-cell suspensions from these tissues were depleted of red blood cells by hypotonic lysis and cytospun onto microscope slides (Fisher Scientific). Peripheral blood smears and single-cell suspensions from spleen and bone marrow were then analyzed by Giemsa/Wright staining using the HEMA solution as per manufacturer's protocol (Biochemical Sciences, Inc., New Jersey).

RNA and PCR analysis

An RT-PCR method was used to measure the G2A RNA levels as previously described (Weng et al., 1998). In brief, total RNA was isolated from either wild-type or G2A-deficient BCR-ABL-transformed leukemic cells from bone marrow or spleen. First-strand cDNA was synthesized from 5 μg of total RNA, using the Superscript preamplification system (GIBCO/BRL). Using G2A-specific primers P1 (TAGCGGTCGCAGGAAATGCAG) and P2 (CAG GACTGGCTTGGGTCATT), 10% of the first-strand cDNA synthesis product was subsequently used for PCR. Glyceraldehyde 3-phosphate dehydrogenase (G3PDH) control amplimer set (CLONTECH) was included as a control to ensure equivalent template levels and quality of RNA.

Cell surface staining and flow cytometric analysis

Single-cell suspensions from spleen, bone marrow and blood, were prepared as described above and stained with combinations of the following antibodies from PharMingen (San Diego, CA), unless otherwise stated: PE-conjugated anti-BP-1, PE-conjugated anti-CD43, PE-conjugated anti-Thy1.2, PE-conjugated anti-Ter119, PE-conjugated anti-Gr1, and Tri-color-conjugated anti-B220 (CALTAG, Burlingame, CA). Data was acquired on a FACScan (Becton Dickinson) and analyzed using CellQuest software. Live cells were gated based on forward and side scatter (Le et al., 2001).

PET imaging

9-(4-[^{18}F]-fluoro-3 hydroxymethylbutyl)guanine (FHBG), a substrate for the HSV1-sr39TK enzyme, was synthesized as previously described (Yaghoubi et al., 2001). At day 9, 16, 23, and 30 posttransplantation, mice were imaged by using the microPET scanner developed at the Crump Institute for Biological Imaging (UCLA) (also available through Concorde Microsystems, Knoxville, TN) (Cherry and Gambhir, 2001). Mice were tail-vein injected with ~200 μCi of FHBG 30 min prior to anesthetization by intraperitoneal injection of 40 μl of a ketamine and xylazine (4:1) solution. Mice were then placed in a spread-prone position on a 8 × 12 cm board and scanned by microPET. Acquisition time was 56 min (8 min per bed position, seven bed positions total), and images were reconstructed by using an interative three-dimensional reconstruction technique as described previously (Qi et al., 1998). At the end of the microPET scan series, animals were sacrificed and detection of leukemic cells in different organs verified the locations of the signals on microPET.

Acknowledgments

We thank Dr. S. Larry Zipursky and members of the Witte lab and Gambhir lab for helpful discussions; James Johnson, Jami McLaughlin, and Shirley Quan for expert technical help; and J.C. White for assistance in the preparation of this manuscript. We are grateful to Dr. Michael Phelps and Dr. Harvey Herschman for introducing us to the benefits of PET reporter gene analysis. L.Q.L. is a Fellow of the University of California, Los Angeles, Medical Scientist Training Program, and supported by a USHHS Institutional National Research Service Award #T32 CA090576 and the Medical Scientist Training Program training grant. J.H.S.K. is a Fellow of the Leukemia and Lymphoma Society (formerly the Leukemia Society of America). O.N.W. is an Investigator of the Howard Hughes Medical Institute. This work was partially supported by NIH grant CA76204 to O.N.W. Imaging described in this paper was supported by funding from DOE contract DE-FC03-87ER60615 (SSG), NIH RO1 CA82214-01 (SSG), and SAIRP R24 CA92865 (SSG).

Received: April 9, 2002
Revised: April 25, 2002

References

Abelson, H.T., and Rabstein, L.S. (1970). Lymphosarcoma: Virus-induced thymic-independent disease in mice. Cancer Res. *30*, 2213–2222.

Afar, D.E.H., Han, L., McLaughlin, J., Wong, S., Dhaka, A., Parmar, K., Rosenberg, N., Witte, O.N., and Colicelli, J. (1997). Regulation of the oncogenic activity of BCR-ABL by a tightly bound substrate protein RIN1. Immunity *6*, 773–782.

Balmain, A. (2002). Cancer as a complex genetic trait. Tumor susceptibility in humans and mouse models. Cell *108*, 145–152.

Cherry, S.R., and Gambhir, S.S. (2001). Use of positron emission tomography in animal research. ILAR J. *42*, 219–232.

Choi, J.W., Lee, S.Y., and Choi, Y. (1996). Identification of a putative G protein-coupled receptor induced during activation-induced apoptosis of T cells. Cell. Immunol. *168*, 78–84.

Chopra, R., Pu, Q.Q., and Elefanty, A.G. (1999). Biology of BCR-ABL. Blood Rev. *13*, 211–229.

Cooper, M.D., Mulvaney, D., Coutinho, A., and Cazenave, P.A. (1986). A novel cell surface molecule on early B-lineage cells. Nature *321*, 616–618.

Cormier, R.T., Hong, K.H., Halberg, R.B., Hawkins, T.L., Richardson, P., Mulherkar, R., Dove, W.F., and Lander, E.S. (1997). Secretory phospholipase Pla2g2a confers resistance to intestinal tumorigenesis. Nat. Genet. *17*, 88–91.

Custer, R.P., Bosma, G.C., and Bosma, M.J. (1985). Severe combined immunodeficiency (SCID) in the mouse. Pathology, reconstitution, neoplasms. Am. J. Pathol. *120*, 464–477.

Dietrich, W.F., Lander, E.S., Smith, J.S., Moser, A.R., Gould, K.A., Luongo, C., Borenstein, N., and Dove, W. (1993). Genetic identification of Mom-1, a major modifier locus affecting Min-Induced intestinal neoplasia in the mouse. Cell *75*, 631–639.

Druker, B.J., and Lydon, N.B. (2000). Lessons learned from the development of an abl tyrosine kinase inhibitor for chronic myelogenous leukemia. J. Clin. Invest. *105*, 3–7.

Gambhir, S.S., Bauer, E., Black, M.E., Liang, Q., Kokoris, M.S., Barrio, J.R., Iyer, M., Namavari, M., Phelps, M.E., and Herschman, H.R. (2000). A mutant herpes simplex virus type 1 thymidine kinase reporter gene shows improved sensitivity for imaging reporter gene expression with positron emission tomography. Proc. Natl. Acad. Sci. USA *97*, 2785–2790.

Gishizky, M.L., and Witte, O.N. (1992). Initiation of deregulated growth of multipotent progenitor cells by bcr-abl in vitro. Science *256*, 836–839.

Gordon, M.Y., Dowding, C.R., Riley, G.P., Goldman, J.M., and Greaves, M.F. (1987a). Altered adhesive interactions with marrow stroma of haematopoietic progenitor cells in chronic myeloid leukaemia. Nature *328*, 342–344.

Gordon, M.Y., Riley, G.P., Watt, S.M., and Greaves, M.F. (1987b). Compartmentalization of a haematopoietic growth factor (GM-SCF) by glycosaminoglycans in the bone marrow microenvironment. Nature *326*, 403–405.

Gorre, M.E., Mohammed, M., Ellwood, K., Hsu, N., Paquette, R., Rao, P.N., and Sawyers, C.L. (2001). Clinical resistance to STI-571 cancer therapy caused by BCR-ABL gene mutation or amplification. Science *293*, 876–880.

Hardy, R.R., and Hayakawa, K. (2001). B cell development pathways. Annu. Rev. Immunol. *19*, 595–621.

Hawley, R.G., Lieu, F.H.L., Fong, Z.C., and Hawley, T.S. (1994). Versatile retroviral vectors for potential use in gene therapy. Gene Ther. *1*, 136–138.

Heiber, M., Docherty, J.M., Shah, G., Nguyen, T., Cheng, R., Heng, H.H., Marchese, A., Tsui, L.C., Shi, X., George, S.R., and O'Dowd, B.F. (1995). Isolation of three novel human genes encoding G protein-coupled receptors. DNA Cell Biol. *14*, 25–35.

Herschman, H.R., MacLaren, D.C., Iyer, M., Namavari, M., Bobinski, K., Green, L.A., Wu, L., Berk, A.J., Toyokuni, T., Barrio, J.R., et al. (2000). Seeing is believing: Non-invasive, quantitative and repetitive imaging of reporter gene expression in living animals, using positron emission tomography. J. Neurosci. Res. *59*, 699–705.

Houlston, R.S., and Tomlinson, I.P. (1998). Modifier genes in humans: strategies for identification. Eur. J. Hum. Genet. *6*, 80–88.

Im, D.S., Heise, C.E., Nguyen, T., O'Dowd, B.F., and Lynch, K.R. (2001). Identification of a molecular target of psychosine and its role in globoid cell formation. J. Cell Biol. *153*, 429–434.

Kabarowski, J.H.S., Feramisco, J.D., Le, L.Q., Gu, J.L., Luoh, S.W., Simon, M.I., and Witte, O.N. (2000). Direct genetic demonstration of G alpha 13 coupling to the orphan G protein-coupled receptor G2A leading to Rho-A-dependent actin rearrangement. Proc. Natl. Acad. Sci. USA *97*, 12109–12114.

Kabarowski, J.H.S., Zhu, K., Le, L.Q., Witte, O.N., and Xu, Y. (2001). Lysophosphatidylcholine is a high affinity ligand for the immunoregulatory receptor G2A. Science *293*, 702–705.

Krebs, D.L., and Hilton, D.J. (2001). SOCS proteins: negative regulators of cytokine signaling. Stem Cells *19*, 378–387.

Kyaw, H., Zeng, Z., Su, K., Fan, P., Shell, B.K., Carter, K.C., and Li, Y. (1998). Cloning, characterization, and mapping of human homolog of mouse T-cell death-associated gene. DNA Cell Biol. *17*, 493–500.

Le, L.Q., Kabarowski, J.H.S., Weng, Z., Satterthwaite, A.B., Harvill, E.T., Jensen, E.R., Miller, J.F., and Witte, O.N. (2001). Mice lacking the orphan G protein-coupled receptor, G2A, develop a late-onset autoimmune syndrome. Immunity *14*, 561–571.

Lim, Y.-M., Wong, S., Lau, G., Witte, O.N., and Colicelli, J. (2000). BCR/ABL inhibition by an escort/phosphatase fusion protein. Proc. Natl. Acad. Sci. USA *97*, 12233–12238.

Lugo, T.G., Pendergast, A., Muller, A.J., and Witte, O.N. (1990). Tyrosine kinase activity and transformation potency of bcr-abl oncogene products. Science *247*, 1079–1082.

McLaughlin, J., Chianese, E., and Witte, O.N. (1987). In vitro transformation of immature hematopoietic cells by the P210 BCR/ABL oncogene product of the Philadelphia chromosome. Proc. Natl. Acad. Sci. USA *84*, 6558–6562.

McLaughlin, J., Chianese, E., and Witte, O.N. (1989). Alternative forms of the BCR-ABL oncogene have quantitatively different potencies for stimulation of immature lymphoid cells. Mol. Cell. Biol. *9*, 1866–1874.

McWhirter, J.R., and Wang, J.Y.J. (1993). An actin-binding function contributes to transformation by the bcr-abl oncoprotein of philadelphia chromosome-positive human leukemias. EMBO J. *12*, 1533–1546.

Mitelman, F. (1993). The cytogenetic scenario of chronic myeloid leukemia. Leuk. Lymphoma *11*, 11–15.

Mock, B.A., Krall, M.M., and Dosik, J.K. (1993). Genetic mapping of tumor

susceptibility genes involved in mouse plasmacytomagenesis. Proc. Natl. Acad. Sci. USA *90*, 9499–9503.

Muller, A.J., Young, J.C., Pendergast, A.-M., Pondel, M., Landau, N.R., Littman, D.R., and Witte, O.N. (1991). BCR first exon sequences specifically activate Bcr/Abl tyrosine kinase oncogene of Philadelphia chromosome positive human leukemias. Mol. Cell. Biol. *11*, 1785–1792.

Nadeau, J.H. (2001). Modifier genes in mice and humans. Nat. Rev. Genet. *2*, 165–174.

Nakao, A., Afrakhte, M., Moren, A., Nakayama, T., Christian, J.L., Heuchel, R., Itoh, S., Kawabata, M., Heldin, N.E., Heldin, C.H., and ten Dijke, P. (1997). Identification of Smad7, a TGFbeta-inducible antagonist of TGF-beta signalling. Nature *389*, 631–635.

Nobes, C.D., and Hall, A. (1995). Rho, Rac, and Cdc42 GTPases regulate the assembly of multimolecular focal complexes associated with actin stress fibers, lamellipodia, and filopodia. Cell *81*, 53–62.

Nowell, P.C., and Hungerford, D.A. (1960). A minute chromosome in human chronic granulocytic leukemia. Science *132*, 1497.

Qi, J., Leahy, R.M., Cherry, S.R., Chatziioannou, A., and Farquhar, T.H. (1998). High-resolution 3D Bayesian image reconstruction using the microPET small-animal scanner. Phys. Med. Biol. *43*, 1001–1013.

Risser, R., Potter, M., and Rowe, W.P. (1978). Abelson virus-induced lymphomagenesis in mice. J. Exp. Med. *148*, 714–726.

Risser, R., Kaehler, D., and Lamph, W.W. (1985). Different genes control the susceptibility of mice to Moloney or Abelson murine leukemia viruses. J. Virol. *55*, 547–553.

Rosenberg, N., and Baltimore, D. (1976). A quantitative assay for transformation of bone marrow cells by Abelson murine leukemia virus. J. Exp. Med. *143*, 1453–1463.

Rowley, J.D. (1973). A new consistent chromosomal abnormality in chronic myelogeneous leukemia identified by quinacrine fluorescence and giemsa staining. Nature *243*, 290–293.

Saglio, G., Guerrasio, A., Rosso, C., Zaccaria, A., Tassinari, A., Serra, A., Rege-Cambrin, G., Mazza, U., and Gavosto, F. (1990). New type of Bcr/Abl junction in Philadelphia chromosome-positive chronic myelogenous leukemia. Blood *76*, 1819–1824.

Sander, E.E., ten Klooster, J.P., van Delft, S., van der Kammen, R.A., and Collard, J.G. (1999). Rac downregulates Rho activity: reciprocal balance between both GTPases determines cellular morphology and migratory behavior. J. Cell Biol. *147*, 1009–1022.

Sawyers, C.L. (1999). Chronic myeloid leukemia. N. Engl. J. Med. *340*, 1330–1340.

Skorski, T., Wlodarski, P., Daheron, L., Salomoni, P., Nieborowska-Skorska, M., Majewski, M., Wasik, M., and Calabretta, B. (1998). BCR/ABL-mediated leukemogenesis requires the activity of the small GTP-binding protein Rac. Proc. Natl. Acad. Sci. USA *95*, 11858–11862.

Stripecke, R., Skelton, D.C., Gruber, T., Afar, D., Pattengale, P.K., Witte, O.N., and Kohn, D.B. (1998). Immune response to Philadelphia chromosome-positive acute lymphoblastic leukemia induced by expression of CD80, interleukin *2,* and granulocyte-macrophage colony-stimulating factor. Hum. Gene Ther. *9*, 2049–2062.

Unnikrishnan, I., Radfar, A., Jenab-Wolcott, J., and Rosenberg, N. (1999). p53 mediates apoptotic crisis in primary Abelson virus-transformed pre-B cells. Mol. Cell. Biol. *19*, 4825–4831.

Van Dyke, T., and Jacks, T. (2002). Cancer modeling in the modern era. Progress and challenges. Cell *108*, 135–144.

Weng, Z., Fluckiger, A.C., Nisitani, S., Wahl, M.I., Le, L.Q., Hunter, C.A., Fernal, A.A., Le Beau, M.M., and Witte, O.N. (1998). A DNA damage and stress inducible G protein-coupled receptor blocks cells in G2/M. Proc. Natl. Acad. Sci. USA *95*, 12334–12339.

Xu, Y., and Casey, G. (1996). Identification of human OGR1, a novel G protein-coupled receptor that maps to chromosome 14. Genomics *5*, 397–402.

Xu, Y., Zhu, K., Hong, G., Wu, W., Baudhuin, L.M., Xiao, Y., and Damron, D.S. (2000). Sphingosylphosphorylcholine is a ligand for ovarian cancer G-protein-coupled receptor 1. Nat. Cell Biol. *2*, 261–267.

Yaghoubi, S., Barrio, J.R., Dahlbom, M., Iyer, M., Namavari, M., Satyamurthy, N., Goldman, R., Herschman, H.R., Phelps, M.E., and Gambhir, S.S. (2001). Human pharmacokinetic and dosimetry studies of [(18)F]FHBG: a reporter probe for imaging herpes simplex virus type-1 thymidine kinase reporter gene expression. J. Nucl. Med. *42*, 1225–1234.

Zhang, S.L., DuBois, W., Ramsay, E.S., Bliskovski, V., Morse, H.C., Taddesse-Heath, L., Vass, W.C., DePinho, R.A., and Mock, B.A. (2001). Efficiency alleles of the Pctr1 modifier locus for plasmacytoma susceptibility. Mol. Cell. Biol. *21*, 310–318.

Zhu, K., Baudhuin, L.M., Hong, G., Williams, F.S., Cristina, K.L., Kabarowski, J.H.S., Witte, O.N., and Xu, Y. (2001). Sphingosylphosphorylcholine and Lysophosphatidylcholine are ligands for the G Protein-coupled receptor GPR4. J. Biol. Chem. *276*, 41325–41335.